Emergent Mott insulators at noninteger fillings and devil's staircase induced by attractive interaction in many-body polarons

Jian-Hua Zeng,[1,2] Su Yi,[3,4,5,*] and Liang He[1,6,†]

[1]*Institute for Theoretical Physics, SPTE, South China Normal University, Guangzhou 510006, China*
[2]*Guangdong Provincial Key Laboratory of Quantum Engineering and Quantum Materials, Guangzhou 510006, China*
[3]*CAS Key Laboratory of Theoretical Physics, Institute of Theoretical Physics, Chinese Academy of Sciences, Beijing 100190, China*
[4]*School of Physical Sciences and CAS Center for Excellence in Topological Quantum Computation, University of Chinese Academy of Sciences, Beijing 100049, China*
[5]*Peng Huanwu Collaborative Center for Research and Education, Beihang University, Beijing 100191, China*
[6]*Guangdong Provincial Key Laboratory of Quantum Engineering and Quantum Materials, Guangdong-Hong Kong Joint Laboratory of Quantum Matter, South China Normal University, Guangzhou 510006, China*

(Received 31 October 2022; revised 18 April 2023; accepted 23 May 2023; published 15 June 2023)

We investigate the ground-state properties of an ultracold-atom system consisting of many-body polarons, quasiparticles formed by impurity atoms in optical lattices immersed in a Bose-Einstein condensate. We find the nearest-neighbor attractive interaction between polarons can give rise to rich physics that is peculiar to this system. In a relatively shallow optical lattice, the attractive interaction can drive the system to be in a self-bound superfluid phase, with its particle density distribution manifesting a self-concentrated structure. However, in a relatively deep optical lattice, the attractive interaction can drive the system, leading to the Mott-insulator phase even though the global filling factor is not an integer. Interestingly, in the Mott-insulator regime, the system can support a series of different Mott insulators, with their effective density manifesting a devil's-staircase structure with respect to the strength of the attractive interaction. A detailed estimation of the relevant experimental parameters shows that these rich physics can be readily observed in current experimental setups.

DOI: 10.1103/PhysRevA.107.063309

I. INTRODUCTION

Since the concept of polarons was first proposed by Landau and Pekar in their study on moving electrons in dielectric crystals [1], understanding the properties of impurities interacting with quantum baths has been an important research field in condensed-matter physics. This is mainly due to the fact that polarons can play an important role in understanding the properties of various important condensed-matter systems such as high-T_c superconductors [2,3] and semiconductors [4,5]; they also naturally attract much research interest in the context of quantum simulations with ultracold atomic gases, for which continuous effort has been devoted to the investigation of polaron physics over the last two decades [6–38].

In this context, single- and few-polaron systems have largely been studied, and their rich physics has been revealed [39–41]. Particularly, the high tunability of optical lattices also motivates investigations of polarons in optical lattices, i.e., polarons formed by impurity atoms in optical lattices immersed in a Bose-Einstein condensate (BEC) [42–45], or coupled to another species of atoms in optical lattices [46–48], where interesting phenomena such as clustering, the self-trapping effect, polaronic slowing, strong influences on polaronic properties imposed by the bath near its phase transition, and the formation of bipolarons have been found.

However, despite these rich physics revealed in single- and few-polaron systems [39–41], the physics associated with many-polaron systems has been far less studied, although the existence of induced effective interactions between polarons has been revealed [42–45,49]. In fact, for polarons in optical lattices, these induced effective interactions not only assume an on-site part but also assume an off-site part. This reminds one of the rich many-body physics of ultracold gases with dipolar interactions in optical lattices (see, e.g., Ref. [50] and references therein). For instance, the so-called devil's staircase, which was first identified in long-range interacting lattice models of classical particles and spins [51–54] and was later also found in other systems, such as liquid crystals [55], quantum models of dimers [56,57], spin-valve systems [58], and fractional quantum Hall systems [59], is identified in ultracold gases with dipolar interactions in optical lattices [60–63].

In these regards, one naturally expects that the induced effective interactions in many-polaron systems could give rise to novel physics that is absent in single- and few-polaron systems. Particularly, in many cases, since the quantum bath that directly interacts with impurity atoms consists of quantum harmonic oscillators, these induced interactions between polarons are usually attractive [42–45,49]. Noticing in addition that polarons in ultracold atomic systems also inherit the repulsive contact interaction from the impurity atoms, this

*syi@itp.ac.cn
†liang.he@scnu.edu.cn

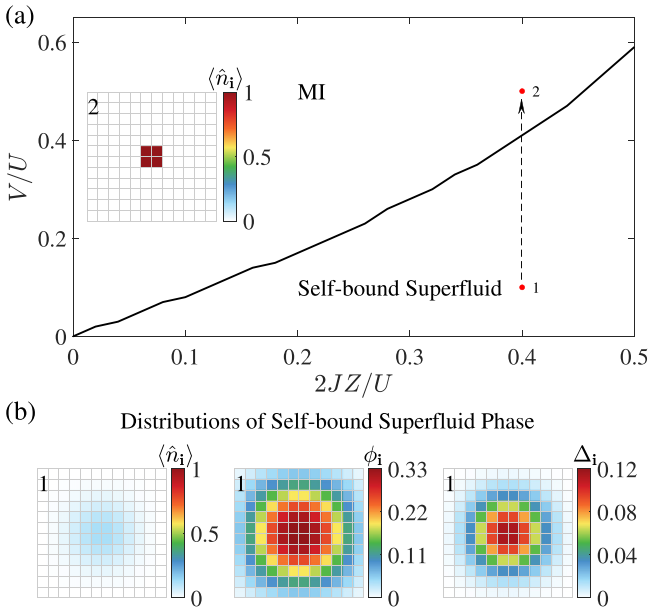

FIG. 1. Phase diagram and typical real-space distributions of the system at the filling factor $\rho = 1/36$ on a 12×12 square lattice. (a) Phase diagram at $\rho = 1/36$, which features a transition between the self-bound superfluid phase and the Mott-insulator (MI) phase. Inset: Real-space polaron density $\langle\hat{n}_i\rangle$ distribution of a MI [upper red dot in main panel, $2JZ/U = 0.4, V/U = 0.5$]. (b) Typical $\langle\hat{n}_i\rangle$, ϕ_i, and Δ_i distributions of the self-bound superfluid [lower red dot in (a), $2JZ/U = 0.4, V/U = 0.1$], featuring a self-concentrated structure. See text for more details.

thus naturally gives rise to the interesting question of physical influences from the competition between these two types of interactions in many-body polarons.

Motivated by recent ultracold-atom experiments, here, we address this question by investigating a system in which one species of bosonic atoms (impurities) trapped in an optical lattice is immersed in a BEC formed by another species of atoms. The interaction between the impurity atoms and the Bogoliubov (phonon) modes of the BEC drives the formation of polarons and gives rise to an interacting many-body polaron system. We investigate the physical influences of the attractive interaction between polarons by establishing the phase diagrams of the system at different filling factors (see Figs. 1 and 2) and find that the attractive interaction can give rise to rich physics. More specifically, we find the following.

(i) We see self-bound superfluids and emergent Mott insulators (MIs) at noninteger filling factors. In a relatively shallow optical lattice, the attractive interaction can drive the system to be in a self-bound superfluid phase, with its particle density distribution manifesting a self-concentrated structure [see Fig. 1(b)]. However, in a relatively deep optical lattice, the attractive interaction can drive the system, forming the Mott-insulator phase even though the global filling factor is not an integer [see the inset of Fig. 1(a)].

(ii) We also see the reentrance to the self-bound superfluid and a devil's staircase induced by attractive interaction. At intermediate filling factors and in the relatively small hopping regime, increasing the attractive interaction strength can

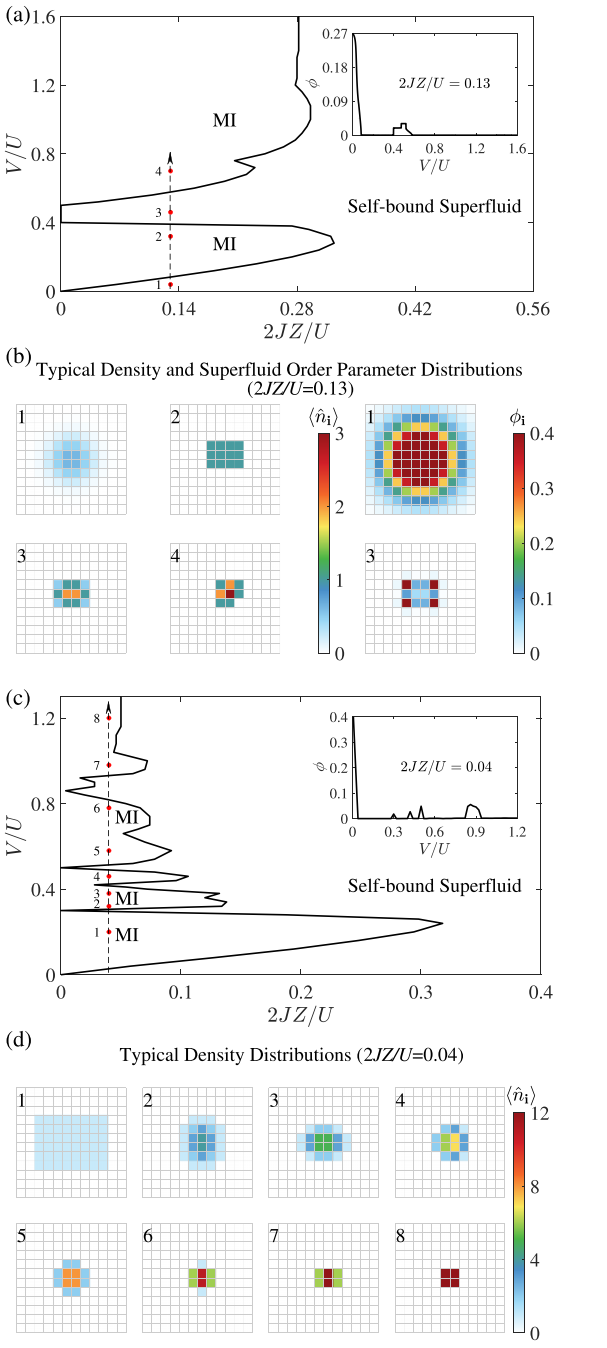

FIG. 2. Phase diagrams and typical real-space distributions at intermediate fillings. (a) Phase diagram at $\rho = 1/12$. The inset shows the V/U dependence of the average superfluid order parameter $\phi \equiv N_{\text{lat}}^{-1} \sum_i \phi_i$ at a fixed hopping amplitude ($2JZ/U = 0.13$; see also the arrow in the main plot). (b) Typical density and superfluid order parameter distributions that correspond to the red dots in (a). The values of V/U for the red dots marked by 1 to 4 are 0.04, 0.32, 0.46, and 0.7, respectively. The $2JZ/U$ values for these dots are the same, with $2JZ/U = 0.13$. (c) Phase diagram at $\rho = 1/3$. The inset shows the V/U dependence of ϕ at a fixed hopping amplitude ($2JZ/U = 0.04$; see also the arrow in the main plot). (d) Density distributions that correspond to the red dots in (c). The values of V/U for the red dots marked by 1 to 8 are 0.2, 0.32, 0.38, 0.46, 0.58, 0.78, 0.98, and 1.2, respectively. The $2JZ/U$ values for these dots are the same, with $2JZ/U = 0.04$. See text for more details.

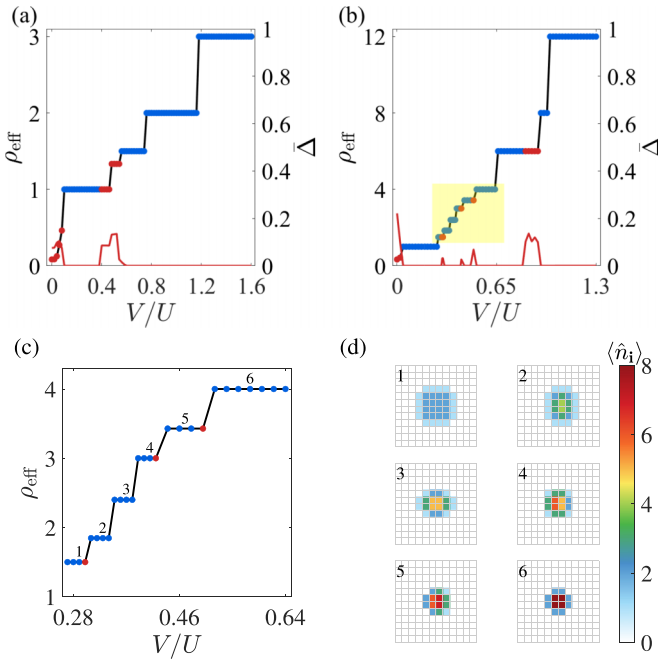

FIG. 3. Devil's staircase induced by the attractive interaction at fixed filling factors. (a) Devil's staircase at a fixed filling factor $\rho = 1/12$. At a hopping amplitude ($2JZ/U = 0.13$), the V/U dependence of the effective density $\rho_{\rm eff}$ (blue and red dots) manifests a series of plateaus. In particular, in the large part of these plateaus marked in blue, the system is in the incompressible Mott-insulator state, as shown by the red solid curve, which is the V/U dependence of the spatially averaged local density fluctuation $\bar{\Delta} \equiv N_{\rm lat}^{-1} \sum_{\mathbf{i}} \Delta_{\mathbf{i}}$. (b) Devil's staircase at the filling factor $\rho = 1/3$ ($2JZ/U = 0.04$). (c) Devil's staircase after zooming in on the yellow region in (b). (d) Density distributions that correspond to the blue part of each plateau in (c). See text for more details.

first drive the system from the self-bound superfluid phase into the Mott-insulator phase, then back to the self-bound superfluid phase again [see the vertical arrows and insets in Figs. 2(a) and 2(c)]. In fact, a series of this type of reentrance can be present in the system as long as the filling factor is large enough [see, for instance, the vertical arrow and inset in Fig. 2(c) with the corresponding filling factor $\rho = 1/3$]. Interestingly, the system can also support a succession of incompressible Mott-insulator states, dense in the parameter space (see Fig. 3), which is reminiscent of the devil's staircase in a long-range interacting system tuned by the filling factor, but here, in our case, it is driven by an essentially short-range attractive interaction with the filling factor of the system kept fixed.

II. SYSTEM AND MODEL

Motivated by related experiments, we consider a system where one species of bosonic atoms (impurities) trapped in a square optical lattice is immersed in a BEC formed by another species of atoms [42,45,64]. The system can be described by a Hamiltonian $\hat{H}_{\rm sys}$ consisting of three parts, i.e., $\hat{H}_{\rm sys} = \hat{H}_I + \hat{H}_B + \hat{H}_{\rm int}$. Here, $\hat{H}_I$ is the Hamiltonian of the impurity atoms assuming the form of a conventional Bose-Hubbard model, i.e., $\hat{H}_I = -\sum_{\langle \mathbf{i},\mathbf{j}\rangle} J_0 \hat{a}_{\mathbf{i}}^\dagger \hat{a}_{\mathbf{j}} - \sum_{\mathbf{i}} \mu_0 \hat{a}_{\mathbf{i}}^\dagger \hat{a}_{\mathbf{i}} + \sum_{\mathbf{i}} (U_0/2) \hat{a}_{\mathbf{i}}^\dagger \hat{a}_{\mathbf{i}}^\dagger \hat{a}_{\mathbf{i}} \hat{a}_{\mathbf{i}}$, with $\hat{a}_{\mathbf{i}}^\dagger$ ($\hat{a}_{\mathbf{i}}$) being the impurity creation (annihilation) operator at site $\mathbf{i}$ in the Wannier basis. The BEC is treated as a Bogoliubov phonon bath described by $\hat{H}_B = \sum_{\mathbf{q}} \hbar \omega_{\mathbf{q}} \hat{\beta}_{\mathbf{q}}^\dagger \hat{\beta}_{\mathbf{q}}$, where $\omega_{\mathbf{q}}$ is the Bogoliubov phonon spectrum with momenta $\mathbf{q}$ and $\hat{\beta}_{\mathbf{q}}^\dagger$ ($\hat{\beta}_{\mathbf{q}}$) is the creation (annihilation) operator for the Bogoliubov phonons. The interaction between the impurities and phonons are described by the Hamiltonian $\hat{H}_{\rm int} = \sum_{\mathbf{i}} \sum_{\mathbf{q}} \hbar \omega_{\mathbf{q}} M_{\mathbf{q}} e^{i\mathbf{q}\cdot\mathbf{r}_{\mathbf{i}}} (\hat{\beta}_{\mathbf{q}} + \hat{\beta}_{-\mathbf{q}}^\dagger) \hat{a}_{\mathbf{i}}^\dagger \hat{a}_{\mathbf{i}} + \text{H.c.}$, where $M_{\mathbf{q}}$ describes the impurity-phonon coupling (see the Appendix for details).

Due to the interactions between the impurity atoms and the Bogoliubov (phonon) modes of the BEC, the impurities and the phonons can form quasiparticles, i.e., polarons [42,45,64]. Using the Lang-Firsov polaron transformation [42,45,64,65], which takes the form $\widetilde{H} \equiv e^{\hat{S}} \hat{H}_{\rm sys} e^{-\hat{S}}$, with $\hat{S} \equiv \sum_{\mathbf{i},\mathbf{q}} \lambda_{\mathbf{q}} M_{\mathbf{q}} e^{i\mathbf{q}\cdot\mathbf{r}_{\mathbf{i}}} (\hat{\beta}_{-\mathbf{q}}^\dagger - \hat{\beta}_{\mathbf{q}}) \hat{a}_{\mathbf{i}}^\dagger \hat{a}_{\mathbf{i}}$, where $\lambda_{\mathbf{q}}$ is the variational parameter of the Lang-Firsov polaron transformation to be determined self-consistently (see the Appendix for details), the transformed Hamiltonian $\widetilde{H}$ can be separated into a coherent part $\langle \widetilde{H} \rangle$ and an incoherent part. At low temperatures, the physics of the system can be effectively described by the coherent part of the Hamiltonian for the polarons after the Lang-Firsov polaron transformation since the incoherent part is strongly suppressed in the low-temperature regime [42,45,64].

Therefore, the effective Hamiltonian for the polarons reads (see the Appendix for more derivation details)

$$\hat{H} = -J \sum_{\langle \mathbf{i},\mathbf{j}\rangle} \hat{b}_{\mathbf{i}}^\dagger \hat{b}_{\mathbf{j}} + \frac{U}{2} \sum_{\mathbf{i}} \hat{n}_{\mathbf{i}} (\hat{n}_{\mathbf{i}} - 1) - \sum_{\langle \mathbf{i},\mathbf{j}\rangle} \frac{V}{2} \hat{n}_{\mathbf{i}} \hat{n}_{\mathbf{j}}, \quad (1)$$

where $\hat{b}_{\mathbf{i}}^\dagger$ ($\hat{b}_{\mathbf{i}}$) is the creation (annihilation) operator of polarons at site $\mathbf{i}$ in the Wannier representation, $\hat{n}_{\mathbf{i}} \equiv \hat{b}_{\mathbf{i}}^\dagger \hat{b}_{\mathbf{i}}$ is the particle number operator that counts the number of polarons on site $\mathbf{i}$, and $\langle \mathbf{i}, \mathbf{j} \rangle$ denotes nearest-neighbor lattice sites. Here, the Hamiltonian (1) assumes the form of the extended Bose-Hubbard model, where the first two terms are the conventional hopping term with hopping amplitude J and the on-site interaction term, whose strength is specified by U. The third term describes the induced nearest-neighbor attractive interaction [42–45,49] between polarons whose strength is specified by V ($V > 0$). It originates from the coupling between impurity atoms and the Bogoliubov modes of the BEC [42,45,64].

From the form of the Hamiltonian (1), we see that its first two terms form the conventional Bose-Hubbard model [66], which favors two homogeneous phases that respect the discrete translational symmetry of the underlying lattice, i.e., homogeneous superfluid at large J/U and homogeneous Mott insulators at integer filling factors at small J/U. However, for the nearest-neighbor attractive interaction term, it can drive the polarons to concentrate in space, making real-space distributions of typical physical quantities, such as density distributions, inhomogeneous. This thus breaks the discrete translational symmetry of the system. In these regards, one would expect that the presence of the nearest-neighbor attractive interaction could give rise to new physics beyond that associated with a conventional superfluid-to-Mott-insulator transition. Indeed, as we shall see in the following, the

attractive interaction can give rise to Mott insulators at noninteger fillings. Even more remarkable, it can drive the system to form a series of incompressible ground states. This is reminiscent of the devil's staircase in long-range interacting systems tuned by the filling factor [51,52,54,61], but here, in our case, it is driven by the attractive interaction, with the filling factor of the system kept fixed.

III. RESULTS

In the investigations that will be presented in the following, we use the bosonic Gutzwiller variational approach [67–69] to investigate the ground-state properties of the system, with the variational ground state assuming the site-factorized form $|\mathrm{GW}\rangle = |\phi_1\rangle_1 \otimes \cdots \otimes |\phi_{N_{\mathrm{lat}}}\rangle_{N_{\mathrm{lat}}}$. Here, N_{lat} is the total number of lattice sites, and $|\phi_{\mathbf{i}}\rangle_{\mathbf{i}} = \sum_{n=0}^{\infty} c_n^{(\mathbf{i})} |n\rangle_{\mathbf{i}}$ is the local wave function at site $\mathbf{i}$, with $|n\rangle_{\mathbf{i}}$ being the corresponding local occupation number state and $c_n^{(\mathbf{i})}$ being the variational parameter. The ground state is determined by minimizing the total energy of the system within this variational ansatz, i.e., $E(\{c_n^{(\mathbf{i})}\}) = \langle \mathrm{GW}|\hat{H}|\mathrm{GW}\rangle$. In the following, we investigate the ground-state properties of the system at different fixed filling factors $\rho \equiv N/N_{\mathrm{lat}}$, with N being the total number of polarons in the system. If not specified in the text, a square lattice with the linear system size $L = 12$, the local occupation number cutoff $n_{\mathrm{max}} = 13$, and open boundary condition are chosen in the numerical results presented in the following (the periodic boundary condition can also be employed and gives rise to only small differences).

A. Self-bound superfluid and emergent Mott insulators at noninteger fillings

At low filling factor $\rho \equiv \langle \hat{N} \rangle / N_{\mathrm{lat}}$, the typical properties of the system are summarized in Fig. 1, which shows a phase diagram of the system at the filling factor $\rho = 1/36$ and typical real-space distributions of polaron density $\langle \hat{n}_{\mathbf{i}} \rangle$, superfluid order parameter $\phi_{\mathbf{i}} \equiv \langle \hat{b}_{\mathbf{i}} \rangle$, and local density fluctuation $\Delta_{\mathbf{i}} \equiv \langle \hat{n}_{\mathbf{i}}^2 \rangle - \langle \hat{n}_{\mathbf{i}} \rangle^2$. In the large-hopping-amplitude regime [see lower right part of Fig. 1(a)], the system breaks the U(1) symmetry and is in a superfluid phase characterized by the existence of the nonzero superfluid order parameter $\phi_{\mathbf{i}}$. Interestingly, as one can see in Fig. 1(b), the polaron density and superfluid order parameter distributions peak at the center of the lattice. We remark here that no external trapping potential is present in our calculation; this real-space concentration reflects the influences of the attractive interaction between polarons. In the following, we thus refer to it as the self-bound superfluid phase.

Compared to conventional homogeneous superfluid phases in similar systems without attractive interactions, the spatial polaron density and superfluid order parameter distributions of the self-bound superfluid phase show that the attractive interaction can drive the polarons to the central region of the system. This indicates that although the filling factor of the system in this case is well below unit filling, a strong enough attractive interaction can still drive the emergence of a local Mott-insulator phase by increasing the local filling factor or density in the central region of the system. Indeed, as one can see from Fig. 1(a), when the attractive interaction strength is relatively strong compared with the hopping amplitude, the system always forms a Mott insulator with a vanishing superfluid order parameter and local density fluctuation. Finally, we remark that because the phase diagrams presented in Figs. 1 and 2 are obtained using the bosonic Gutzwiller variational approach, possibly strong quantum fluctuations that exist in the vicinity of the phase boundaries are not well accounted for within this mean-field approach. These quantum fluctuations are expected to impose corrections on the phase boundaries and local density fluctuations in these quantum critical regimes. Although they are beyond the scope of the current work, it would be interesting to further investigate the influences of quantum fluctuations in these quantum critical regimes by employing methods beyond the mean field, such as the quantum Monte Carlo method [70,71], which has been applied to study Bose-Hubbard-type models and the quantum Gutzwiller approach developed recently [72,73].

B. Reentrance to self-bound superfluid and devil's staircase induced by attractive interaction

Noticing that in the above low-filling case, the total particle number of the system is quite small ($N = 4$) and strongly restricts the number of possible configurations of density distributions, one naturally expects that at intermediate filling factors, the system could manifest richer physics induced by the attractive interaction. This motivates us to investigate the properties of the system at intermediate filling factors, the results of which are summarized in Fig. 2, where two phase diagrams of the system at two different intermediate filling factors ($\rho = 1/12,\ 1/3$) are shown. Compared with the phase diagram at the low filling factor, the ones at intermediate fillings assume a more delicate Mott-insulator to self-bound superfluid transition boundary.

Taking the phase diagram of the system at $\rho = 1/12$, for instance [see Fig. 2(a)], one can see that in the relatively small hopping regime, by increasing the attractive interaction strength, the system first transits from a self-bound superfluid to a Mott insulator, similar to what happens in the above low-filling case; however, it transits back to the self-bound superfluid from the Mott insulator upon further increasing the attractive interaction strength [see the vertical arrow and inset in Fig. 2(a)]. This indicates the attractive interaction can drive a reentrant transition to the self-bound superfluid phase. By comparing the density and superfluid order parameter distributions of the self-bound superfluid phase at weak attractive interaction strength [see the plots labeled 1 in Fig. 2(b)] and those of the reentered self-bound superfluid phase [see the plots labeled 3 in Fig. 2(b)], one notices that the density and superfluid order parameter distributions of the reentered self-bound superfluid are much more compressed due to the stronger attractive interaction. Moreover, further comparing the density distribution of the reentered self-bound superfluid with those of the Mott-insulator phases nearby in the parameter space [see the plots labeled 2 and 4 in Fig. 2(b)], one can see that the extent of compression of the reentered self-bound superfluid is between those of these two Mott insulators. This suggests the reentered self-bound superfluid phase can be regarded as the intermediate phase between two adjacent (in the parameter space) Mott insulators with

different density distributions. Indeed, in the parameter regime where two adjacent Mott insulators have similar energies, one expects the quantum tunneling of polarons between different sites to become much easier, hence giving rise to the reentered self-bound superfluid.

As a matter of fact, at a larger filling factor ($\rho = 1/3$, for instance), the attractive interaction can drive not only one but a series of reentrances to the self-bound superfluid, as shown in Fig. 2(c). This series of reentered self-bound superfluid appears to be intermediate phases between a series of adjacent (in the parameter space) Mott insulators with different density distributions [see Fig. 2(d)].

To effectively characterize this series of Mott insulators and reentrances to the self-bound superfluid in the weak-hopping regime, we introduce the effective density $\rho_{\text{eff}} \equiv N/N_{\text{lat}}^{\text{eff}}$, which describes the average density of the system in the region with nonzero polaron density ($N_{\text{lat}}^{\text{eff}}$ is the number of lattice sites with nonzero density). Figure 3 shows how the effective density changes with respect to the attractive interaction strength at two fixed filling factors with $\rho = 1/12$ and $\rho = 1/3$. We notice that the effective density ρ_{eff} of the system manifests a series of plateaus with respect to the attractive interaction strength, and in the large part of these plateaus marked in blue in Fig. 3, the system is in the incompressible Mott-insulator state. In particular, at the relatively high filling ($\rho = 1/3$, for instance) shown in Figs. 3(b) and 3(c), these plateaus can be quite dense in the parameter space. This is reminiscent of the devil's staircase in systems with long-range repulsive interactions [51–54,60–63,74,75]; therefore, we also refer to this succession of incompressible ground states, dense in the parameter space, as the devil's staircase.

However, we emphasize that there are substantial differences between the devil's staircase found here and those in systems with long-range repulsive interactions [51–54,60–63,74,75]. In the latter, the devil's staircase is driven by changing the chemical potential (or, equivalently, the number of particles in the system); that is, different incompressible ground states that are located on different steps of the staircase correspond to systems with a different particle numbers (or filling factors). However, for the many-body polaron system investigated here, the devil's staircase is driven by the attractive interaction with the number of particles in the system kept fixed; that is, different incompressible ground states that are located on different steps of the staircase correspond to systems with different attractive interaction strengths but with the same particle number. Note also that, for systems with long-range repulsive interactions, the long interaction range (i.e., the strength of the interaction assuming a power-law decay with respect to the distance) is crucial for the development of the chemical-potential-driven devil's staircase [60–63], whereas for the many-body polaron system investigated here, the interaction that drives the emergence of the devil's staircase is essentially short-range since the interaction range covers only nearest-neighbor sites, as shown in Hamiltonian (1). Moreover, the incompressible ground states associated with the devil's staircase in these two cases also manifest distinct spatial structures. For systems with long-range repulsive interactions, the density distributions of these states usually assume density-wave structures commensurate with the underlying lattice [60–63], which is in sharp contrast to the self-concentrated structure in the many-body polaron system [see Fig. 3(d), for instance].

C. Experimental observability

We believe that the physics predicted in this work can be readily observed in current experimental setups. For instance, one could employ an experimental setup similar to the one presented in Ref. [76]. Namely, one could immerse ^{133}Cs impurities, with scattering lengths of $220a_0$ (a_0 denotes the Bohr radius), trapped by laser beams with wavelength $\lambda = 1064$ nm, in a BEC with an average density $n_0 = 1.0 \times 10^{14}$ cm^{-3} formed by ^{87}Rb atoms. By using the Feshbach resonance between ^{133}Cs and ^{87}Rb [77], as shown in Fig. 4 in the Appendix, one could, indeed, tune the ratio between the attractive interaction strength and the on-site repulsive interaction strength, i.e., V/U in the interval (0,1.5) (see the Appendix for estimation details). Moreover, one could also immerse ^{39}K impurities (with scattering lengths of $278a_0$ [78]) in a BEC with an average density $n_0 = 2.3 \times 10^{14}$ cm^{-3} formed by ^{87}Rb atoms [28]. Similarly, by using the Feshbach resonance between ^{39}K and ^{87}Rb [28], as shown in Fig. 4 in the Appendix, one could thus tune the interaction ratio V/U in the interval (0,1.5) to observe the physics predicted here.

Moreover, we believe that the physics predicted here could be relevant for quantum gases consisting of atoms with magnetic dipole moments in square optical lattices, with the attractive interaction in Hamiltonian (1) realized by imposing a magnetic field rotating along a cone centered around the direction perpendicular to the lattice plane [79–81]. Also, Hamiltonian (1) is expected to be relevant for microwave-dressed polar molecules in square optical lattices, where, in particular, the attractive interaction in (1) can be realized by a rotating electric field with the rotating axis perpendicular to the lattice plane [82].

IV. CONCLUSIONS

The competition between the local repulsive interaction and the nearest-neighbor attractive interaction in many-body polarons in optical lattices formed by ultracold atoms can give rise to rich physics, as its phase diagrams at different filling factors have shown: at a relatively large hopping amplitude, the attractive interaction can drive the system to be in a self-bound superfluid phase, with its particle density distribution manifesting a self-concentrated structure. In the relatively small hopping amplitude regime, the attractive interaction can drive the system, forming the Mott-insulator phase even though the global filling factor is not an integer. Interestingly, in the Mott-insulator regime, the system can support a series of different incompressible Mott insulators whose local effective filling factors manifest a devil's-staircase structure with respect to the strength of attractive interaction. A detailed estimation of the relevant experimental parameters showed that these rich physics can be readily observed in current experimental setups [28,76]. We believe our work will stimulate both further theoretical and experimental efforts to reveal the rich physics of many-body polaron systems.

ACKNOWLEDGMENTS

We thank Jiarui Fang and Tao Yin for helpful discussions. This work was supported by the NSFC (Grants No. 11874017, No. 12135018, No. 12047503, and No. 12275089), NKRDPC (Grants No. 2021YFA0718304 and No. 2022YFA1405304), the Guangdong Provincial Key Laboratory (Grant No. 2020B1212060066), the Guangdong Basic and Applied Basic Research Foundation (Grant No. 2023A1515012800), and the START Grant of South China Normal University.

APPENDIX: DERIVATION OF THE EFFECTIVE HAMILTONIAN AND EXPERIMENTAL PARAMETER ESTIMATION

In this Appendix, we present the detailed derivation of the effective Hamiltonian (1) and estimate the region of relevant experimental parameters where the physics predicted in this work can be observed. We consider impurities with mass m_I interacting with a BEC formed by atoms with mass m_B. The impurities are trapped in a relatively deep optical lattice and are described by the Hamiltonian $\hat{H}_I$ presented in the main text. In the following, we use the harmonic approximation for the Wannier basis (at site $\mathbf{0}$ for instance) for the impurity, which assumes the form

$$W(\mathbf{r}) = \frac{1}{(\pi\sigma_\parallel^2)^{\frac{1}{2}}} e^{-\frac{(x^2+y^2)}{2\sigma_\parallel^2}} \left(\frac{\sqrt{n_\perp/n_\parallel}}{\pi\sigma_\parallel^2}\right)^{\frac{1}{4}} e^{-\frac{\sqrt{n_\perp/n_\parallel}}{2\sigma_\parallel^2} z^2}, \tag{A1}$$

with $\sigma_\parallel = \sqrt{\hbar/m_I\omega_\parallel} = d/(\pi n_\parallel^{\frac{1}{4}})$ and oscillation frequency $\hbar\omega_\parallel \equiv 2(V_I^\parallel E_R)^{1/2}$. The trapping strength in the transverse (z) direction $V_I^\perp$ is much stronger than in the parallel (x, y) directions $V_I^\parallel$, with $n_\perp \equiv V_I^\perp/E_R$ and $n_\parallel \equiv V_I^\parallel/E_R$. The on-site interaction and hopping amplitude for the impurities can be obtained, i.e.,

$$\begin{aligned} U_0 &= \frac{g_{\rm II}}{2}\int d^3\mathbf{r}|W(\mathbf{r})|^4 \\ &\approx \sqrt{8\pi}\frac{a_{\rm II}}{d} n_\parallel^{\frac{1}{2}} n_\perp^{\frac{1}{4}} E_R, \end{aligned} \tag{A2}$$

$$J_0 \approx \frac{4}{\sqrt{\pi}} E_R n_\parallel^{\frac{3}{4}} e^{-2\sqrt{n_\parallel}}, \tag{A3}$$

where $d = \lambda/2$ is the lattice constant, λ is the laser wavelength, and $E_R \equiv \hbar^2k^2/(2m_I)$ is the recoil energy with $k = 2\pi/\lambda$. The interaction between impurities is determined by $g_{\rm II} = 4\pi\hbar^2 a_{\rm II}/m_I$, where $a_{\rm II}$ is the scattering length between impurities.

The BEC of ultracold atoms with weak repulsive contact interactions can be described by the Bogoliubov theory and treated as a phonon bath [42,45,64] described by the Hamiltonian $\hat{H}_B$ presented in the main text. The spectrum $\hbar\omega_{\mathbf{q}}$ for the Bogoliubov phonons that appears in $\hat{H}_B$ assumes the explicit form $\hbar\omega_{\mathbf{q}} = \sqrt{\epsilon_{\mathbf{q}}(\epsilon_{\mathbf{q}} + 2g_{\rm BB}n_0)}$, with $\epsilon_{\mathbf{q}} \equiv \hbar^2|\mathbf{q}|^2/(2m_B)$, n_0 being the average BEC density, and $g_{\rm BB}$ being the strength of the repulsive contact interaction determined by the boson-boson scattering length $a_{\rm BB}$ via $g_{\rm BB} = 4\pi\hbar^2 a_{\rm BB}/m_B$.

The impurity-BEC interaction term can be written as the Fröhlich impurity-phonon coupling [45] $\hat{H}_{\rm int}$ presented in the main text, where the explicit form of $M_{\mathbf{q}}$ that appears in $\hat{H}_{\rm int}$ reads

$$M_{\mathbf{q}} = g_{\rm IB}\sqrt{\frac{n_0\epsilon_{\mathbf{q}}}{\Omega(\hbar\omega_{\mathbf{q}})^3}} e^{-\frac{(q_x^2+q_y^2)\sigma_\parallel^2 + q_z^2\sigma_\perp^2}{4}}, \tag{A4}$$

with Ω being the system quantization volume. The interspecies interaction $g_{\rm IB}$ is determined by $g_{\rm IB} = 2\pi\hbar^2 a_{\rm IB}/m_{\rm IB}$, with $m_{\rm IB} = m_I m_B/(m_I + m_B)$ being the reduced mass and $a_{\rm IB}$ being the impurity-boson scattering length.

As presented in the main text, one can use the Lang-Firsov polaron transformation [42,45,64,65] to transform the Hamiltonian of the whole system $\hat{H}_{\rm sys}$ into a Hamiltonian $\tilde{H}$. This transformed Hamiltonian $\tilde{H}$ can be separated into a coherent part $\langle\tilde{H}\rangle$ and an incoherent part. The incoherent part is strongly suppressed in the low-temperature regime $k_BT \ll g_{\rm IB}^2/(2\xi g_{\rm BB})$ [42], with ξ being the condensate healing length. Therefore, to investigate the ground-state properties of the system, one can neglect the incoherent part and focus on the coherent one, which is decoupled from the phonon bath and assumes the form of an extended (polaronic) Hubbard model with phonons eliminated by thermal averaging, i.e.,

$$\begin{aligned} \hat{H}_{\rm P} \equiv \langle\tilde{H}\rangle = &-\sum_{\langle\mathbf{i},\mathbf{j}\rangle} J\hat{b}_{\mathbf{i}}^\dagger\hat{b}_{\mathbf{j}} - \sum_{\mathbf{i}}\mu\hat{n}_{\mathbf{i}} \\ &+ \sum_{\mathbf{i}}\frac{U_0 - V_{\mathbf{i},\mathbf{i}}}{2}\hat{n}_{\mathbf{i}}(\hat{n}_{\mathbf{i}} - 1) - \sum_{\mathbf{i}\neq\mathbf{j}}\frac{V_{\mathbf{i},\mathbf{j}}}{2}\hat{n}_{\mathbf{i}}\hat{n}_{\mathbf{j}}. \end{aligned} \tag{A5}$$

Here, J is the renormalized polaronic hopping, with $J \equiv J_0 e^{-\sum_{\mathbf{q}}(2N_{\mathbf{q}}+1)[1-\cos(\mathbf{q}\cdot\mathbf{d})]|\lambda_{\mathbf{q}}M_{\mathbf{q}}|^2}$ and $\mathbf{d}$ being $d\vec{e}_x$ or $d\vec{e}_y$. μ is the renormalized chemical potential, with $\mu \equiv \mu_0 + \sum_{\mathbf{q}}\omega_{\mathbf{q}}\lambda_{\mathbf{q}}(2 - \lambda_{\mathbf{q}})|M_{\mathbf{q}}|^2$, and $U_0 - V_{\mathbf{i},\mathbf{i}}$ is the on-site interaction strength including the polaron energy shift. The effective off-site interaction strength

$$V_{\mathbf{i},\mathbf{j}} = \sum_{\mathbf{q}}\hbar\omega_{\mathbf{q}}M_{\mathbf{q}}^2\left[\left(2\lambda_{\mathbf{q}} - \lambda_{\mathbf{q}}^2\right) + \text{H.c.}\right]\cos(\mathbf{q}\cdot\mathbf{R}_{\mathbf{ij}}), \tag{A6}$$

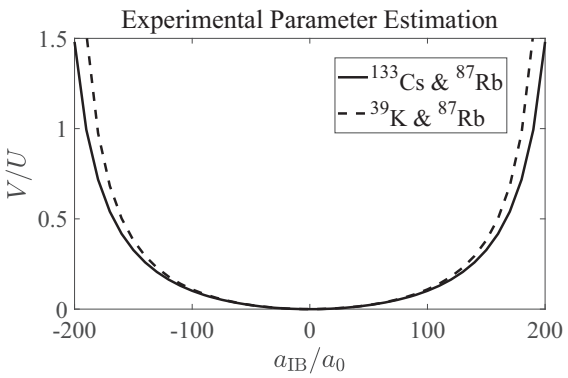

FIG. 4. Estimation of V/U in relevant experimental systems. Solid curve: ^{133}Cs impurities in a BEC formed by ^{87}Rb atoms. Dotted curve: ^{39}K impurities in a BEC formed by ^{87}Rb atoms. By tuning the scattering length between impurity atoms and BEC atoms using Feshbach resonance, the parameter region of V/U in the phase diagrams shown in Figs. 1 and 2 can be achieved in these experimental setups.

where $\mathbf{R_{ij}} \equiv \mathbf{r_i} - \mathbf{r_j}$. Actually, the strength of $V_{\mathbf{i},\mathbf{j}}$ decays very fast with respect to $|\mathbf{R_{ij}}|$ [45]; therefore, we keep only the nearest-neighbor interaction term in the final effective Hamiltonian (1) for the polarons. Moreover, to estimate the value of the parameters appearing in the effective Hamiltonian (1) of the polarons, we further employ a simple momentum-independent ansatz for $\lambda_{\mathbf{q}}$, i.e., $\lambda = \lambda_{\mathbf{q}}$. This momentum-independent ansatz works well in the strong-coupling regime [42], and also there have been investigations showing that the variation of $\lambda_{\mathbf{q}}$ with respect to $\mathbf{q}$ is usually small [45]; therefore, we expect this ansatz could give a reasonably good estimation of the parameters that appear in the effective Hamiltonian of the polarons, particularly in the strong impurity-photon coupling regime that accommodates more interesting physics. In practice, λ is determined by minimizing the ground-state energy [45], and the corresponding self-consistent equation for λ reads

$$\lambda = \left[1 + 2|J_0|\frac{\sum_{\mathbf{q}} f_{\mathbf{q}}|M_{\mathbf{q}}|^2}{\sum_{\mathbf{q}} \hbar\omega_{\mathbf{q}}|M_{\mathbf{q}}|^2} e^{-\lambda^2 \sum_{\mathbf{q}} f_{\mathbf{q}}|M_{\mathbf{q}}|^2}\right]^{-1}, \tag{A7}$$

where $f_{\mathbf{q}} \equiv (2N_{\mathbf{q}} + 1)[1 - \cos(\mathbf{q} \cdot \mathbf{d})]$, with the thermally averaged phonon occupation number $N_{\mathbf{q}} \equiv [e^{\hbar\omega_{\mathbf{q}}/(k_B T)} - 1]^{-1}$.

According to the above expressions for the interaction parameters that appear in the effective Hamiltonian (1), we can estimate the ratio between the attractive interaction strength and the on-site repulsive interaction strength, i.e., V/U. The dependence of this ratio on impurity-boson scattering length a_{IB} is shown in Fig. 4 for two relevant experimental setups (see Sec. III C). One can see that the parameter region of V/U that accommodates the physics predicted here can be achieved by tuning a_{IB} in experiments.

[1] L. Landau and S. Pekar, Zh. Eksp. Teor. Fiz. **18**, 419 (1948).
[2] A. Lanzara, P. Bogdanov, and X. Zhou, Nature (London) **412**, 510 (2001).
[3] P. A. Lee, N. Nagaosa, and X.-G. Wen, Rev. Mod. Phys. **78**, 17 (2006).
[4] M. E. Gershenson, V. Podzorov, and A. F. Morpurgo, Rev. Mod. Phys. **78**, 973 (2006).
[5] N. Lu, L. Li, D. Geng, and M. Liu, Org. Electron. **61**, 223 (2018).
[6] G. E. Astrakharchik and L. P. Pitaevskii, Phys. Rev. A **70**, 013608 (2004).
[7] K. Günter, T. Stöferle, H. Moritz, M. Köhl, and T. Esslinger, Phys. Rev. Lett. **96**, 180402 (2006).
[8] S. Ospelkaus, C. Ospelkaus, O. Wille, M. Succo, P. Ernst, K. Sengstock, and K. Bongs, Phys. Rev. Lett. **96**, 180403 (2006).
[9] F. Chevy, Phys. Rev. A **74**, 063628 (2006).
[10] R. M. Kalas and D. Blume, Phys. Rev. A **73**, 043608 (2006).
[11] F. M. Cucchietti and E. Timmermans, Phys. Rev. Lett. **96**, 210401 (2006).
[12] N. Prokof'ev and B. Svistunov, Phys. Rev. B **77**, 020408 (2008).
[13] A. Schirotzek, C.-H. Wu, A. Sommer, and M. W. Zwierlein, Phys. Rev. Lett. **102**, 230402 (2009).
[14] S. Palzer, C. Zipkes, C. Sias, and M. Köhl, Phys. Rev. Lett. **103**, 150601 (2009).
[15] S. Nascimbène, N. Navon, K. J. Jiang, L. Tarruell, M. Teichmann, J. McKeever, F. Chevy, and C. Salomon, Phys. Rev. Lett. **103**, 170402 (2009).
[16] R. L. Frank, E. H. Lieb, R. Seiringer, and L. E. Thomas, Phys. Rev. Lett. **104**, 210402 (2010).
[17] C. Kohstall, M. Zaccanti, M. Jag, A. Trenkwalder, P. Massignan, G. M. Bruun, F. Schreck, and R. Grimm, Nature (London) **485**, 615 (2012).
[18] Y. Zhang, W. Ong, I. Arakelyan, and J. E. Thomas, Phys. Rev. Lett. **108**, 235302 (2012).
[19] W. Casteels, J. Tempere, and J. T. Devreese, Phys. Rev. A **86**, 043614 (2012).
[20] R. Schmidt, T. Enss, V. Pietilä, and E. Demler, Phys. Rev. A **85**, 021602(R) (2012).
[21] J. Catani, G. Lamporesi, D. Naik, M. Gring, M. Inguscio, F. Minardi, A. Kantian, and T. Giamarchi, Phys. Rev. A **85**, 023623 (2012).
[22] T. Fukuhara, A. Kantian, M. Endres, M. Cheneau, P. Schauß, S. Hild, D. Bellem, U. Schollwöck, T. Giamarchi, C. Gross, I. Bloch, and S. Kuhr, Nat. Phys. **9**, 235 (2013).
[23] S. P. Rath and R. Schmidt, Phys. Rev. A **88**, 053632 (2013).
[24] W. Li and S. Das Sarma, Phys. Rev. A **90**, 013618 (2014).
[25] F. Grusdt, Y. E. Shchadilova, A. N. Rubtsov, and E. Demler, Sci. Rep. **5**, 12124 (2015).
[26] R. S. Christensen, J. Levinsen, and G. M. Bruun, Phys. Rev. Lett. **115**, 160401 (2015).
[27] L. A. Peña Ardila and S. Giorgini, Phys. Rev. A **92**, 033612(R) (2015).
[28] N. B. Jørgensen, L. Wacker, K. T. Skalmstang, M. M. Parish, J. Levinsen, R. S. Christensen, G. M. Bruun, and J. J. Arlt, Phys. Rev. Lett. **117**, 055302 (2016).
[29] M.-G. Hu, M. J. Van de Graaff, D. Kedar, J. P. Corson, E. A. Cornell, and D. S. Jin, Phys. Rev. Lett. **117**, 055301 (2016).
[30] M. Cetina, M. Jag, R. S. Lous, I. Fritsche, J. T. M. Walraven, R. Grimm, J. Levinsen, M. M. Parish, R. Schmidt, M. Knap, and E. Demler, Science **354**, 96 (2016).
[31] Y. E. Shchadilova, R. Schmidt, F. Grusdt, and E. Demler, Phys. Rev. Lett. **117**, 113002 (2016).
[32] F. F. Bellotti, T. Frederico, M. T. Yamashita, D. V. Fedorov, A. S. Jensen, and N. T. Zinner, New J. Phys. **18**, 043023 (2016).
[33] R. Schmidt and M. Lemeshko, Phys. Rev. X **6**, 011012 (2016).
[34] F. Scazza, G. Valtolina, P. Massignan, A. Recati, A. Amico, A. Burchianti, C. Fort, M. Inguscio, M. Zaccanti, and G. Roati, Phys. Rev. Lett. **118**, 083602 (2017).
[35] C. H. Greene, P. Giannakeas, and J. Pérez-Ríos, Rev. Mod. Phys. **89**, 035006 (2017).
[36] S. Van Loon, W. Casteels, and J. Tempere, Phys. Rev. A **98**, 063631 (2018).
[37] M. G. Skou, T. G. Skov, N. B. Jørgensen, K. K. Nielsen, A. Camacho-Guardian, T. Pohl, G. M. Bruun, and J. J. Arlt, Nat. Phys. **17**, 731 (2021).
[38] P. E. Dolgirev, Y.-F. Qu, M. B. Zvonarev, T. Shi, and E. Demler, Phys. Rev. X **11**, 041015 (2021).

[39] R. Schmidt, M. Knap, D. A. Ivanov, J.-S. You, M. Cetina, and E. Demler, Rep. Prog. Phys. **81**, 024401 (2018).
[40] P. Massignan, M. Zaccanti, and G. M. Bruun, Rep. Prog. Phys. **77**, 034401 (2014).
[41] I. Bloch, J. Dalibard, and S. Nascimbène, Nat. Phys. **8**, 267 (2012).
[42] M. Bruderer, A. Klein, S. R. Clark, and D. Jaksch, Phys. Rev. A **76**, 011605(R) (2007).
[43] A. Klein, M. Bruderer, S. R. Clark, and D. Jaksch, New J. Phys. **9**, 411 (2007).
[44] A. Privitera and W. Hofstetter, Phys. Rev. A **82**, 063614 (2010).
[45] T. Yin, D. Cocks, and W. Hofstetter, Phys. Rev. A **92**, 063635 (2015).
[46] V. R. Yordanov and F. Isaule, J. Phys. B **56**, 045301 (2023).
[47] V. E. Colussi, F. Caleffi, C. Menotti, and A. Recati, Phys. Rev. Lett. **130**, 173002 (2023).
[48] S. Ding, G. A. Domínguez-Castro, A. Julku, A. Camacho-Guardian, and G. M. Bruun, SciPost Phys. **14**, 143 (2023).
[49] D. H. Santamore and E. Timmermans, New J. Phys. **13**, 103029 (2011).
[50] M. A. Baranov, M. Dalmonte, G. Pupillo, and P. Zoller, Chem. Rev. **112**, 5012 (2012).
[51] J. Hubbard, Phys. Rev. B **17**, 494 (1978).
[52] M. E. Fisher and W. Selke, Phys. Rev. Lett. **44**, 1502 (1980).
[53] P. Bak and J. von Boehm, Phys. Rev. B **21**, 5297 (1980).
[54] P. Bak and R. Bruinsma, Phys. Rev. Lett. **49**, 249 (1982).
[55] H. Takezoe, E. Gorecka, and M. Čepič, Rev. Mod. Phys. **82**, 897 (2010).
[56] E. Fradkin, D. A. Huse, R. Moessner, V. Oganesyan, and S. L. Sondhi, Phys. Rev. B **69**, 224415 (2004).
[57] T. Schlittler, T. Barthel, G. Misguich, J. Vidal, and R. Mosseri, Phys. Rev. Lett. **115**, 217202 (2015).
[58] T. Matsuda, S. Partzsch, T. Tsuyama, E. Schierle, E. Weschke, J. Geck, T. Saito, S. Ishiwata, Y. Tokura, and H. Wadati, Phys. Rev. Lett. **114**, 236403 (2015).
[59] P. Rotondo, L. G. Molinari, P. Ratti, and M. Gherardi, Phys. Rev. Lett. **116**, 256803 (2016).
[60] F. J. Burnell, M. M. Parish, N. R. Cooper, and S. L. Sondhi, Phys. Rev. B **80**, 174519 (2009).
[61] B. Capogrosso-Sansone, C. Trefzger, M. Lewenstein, P. Zoller, and G. Pupillo, Phys. Rev. Lett. **104**, 125301 (2010).
[62] T. Ohgoe, T. Suzuki, and N. Kawashima, Phys. Rev. A **86**, 063635 (2012).
[63] C. Zhang, J. Zhang, J. Yang, and B. Capogrosso-Sansone, Phys. Rev. A **103**, 043333 (2021).
[64] M. Bruderer, A. Klein, S. R. Clark, and D. Jaksch, New J. Phys. **10**, 033015 (2008).
[65] S. Maier, T. L. Schmidt, and A. Komnik, Phys. Rev. B **83**, 085401 (2011).
[66] M. P. A. Fisher, P. B. Weichman, G. Grinstein, and D. S. Fisher, Phys. Rev. B **40**, 546 (1989).
[67] W. Krauth, M. Caffarel, and J.-P. Bouchaud, Phys. Rev. B **45**, 3137 (1992).
[68] D. Jaksch, C. Bruder, J. I. Cirac, C. W. Gardiner, and P. Zoller, Phys. Rev. Lett. **81**, 3108 (1998).
[69] N. Lanatà, H. U. R. Strand, X. Dai, and B. Hellsing, Phys. Rev. B **85**, 035133 (2012).
[70] B. Capogrosso-Sansone, N. V. Prokof'ev, and B. V. Svistunov, Phys. Rev. B **75**, 134302 (2007).
[71] M. Guglielmino, V. Penna, and B. Capogrosso-Sansone, Phys. Rev. A **82**, 021601(R) (2010).
[72] F. Caleffi, M. Capone, C. Menotti, I. Carusotto, and A. Recati, Phys. Rev. Res. **2**, 033276 (2020).
[73] V. E. Colussi, F. Caleffi, C. Menotti, and A. Recati, SciPost Phys. **12**, 111 (2022).
[74] Z. Lan, J. Minář, E. Levi, W. Li, and I. Lesanovsky, Phys. Rev. Lett. **115**, 203001 (2015).
[75] Z. Lan, I. Lesanovsky, and W. Li, Phys. Rev. B **97**, 075117 (2018).
[76] L. Reichsöllner, A. Schindewolf, T. Takekoshi, R. Grimm, and H.-C. Nägerl, Phys. Rev. Lett. **118**, 073201 (2017).
[77] T. Takekoshi, M. Debatin, R. Rameshan, F. Ferlaino, R. Grimm, H.-C. Nägerl, C. R. Le Sueur, J. M. Hutson, P. S. Julienne, S. Kotochigova, and E. Tiemann, Phys. Rev. A **85**, 032506 (2012).
[78] R. Côté, A. Dalgarno, H. Wang, and W. C. Stwalley, Phys. Rev. A **57**, R4118 (1998).
[79] S. Giovanazzi, A. Görlitz, and T. Pfau, Phys. Rev. Lett. **89**, 130401 (2002).
[80] S. Yi, T. Li, and C. P. Sun, Phys. Rev. Lett. **98**, 260405 (2007).
[81] Y. Tang, W. Kao, K.-Y. Li, and B. L. Lev, Phys. Rev. Lett. **120**, 230401 (2018).
[82] A. Schindewolf, R. Bause, X.-Y. Chen, M. Duda, T. Karman, I. Bloch, and X.-Y. Luo, Nature (London) **607**, 677 (2022).